Evidence for Reptational Motion and the Entanglement Tube in Semidilute Polymer Solutions

Paul T. Callaghan and Andrew Coy
Department of Physics and Biophysics, Massey University, Palmerston North, New Zealand

(Received 3 December 1991)

The internal dynamics of high molar mass polystyrene in semidilute solution have been examined using pulsed gradient spin echo NMR. We find evidence for reptationlike motion characterized by mean-square displacement $\phi(t) \sim t^{1/4}$, $t^{1/2}$, and t regimes. We observe clear transitions between $\phi(t) \sim t^{1/2}$ and $\phi(t) \sim t$ regimes and the data are broadly consistent with the quantitative predictions of Doi-Edwards theory. In an experiment akin to dynamic neutron scattering, we obtain a structure factor from which some information about entanglement tube dimensions can be deduced.

PACS numbers: 61.25.Hq

A central question in understanding the dynamics of entangled polymer molecules concerns whether linear chains in semidilute solution undergo reptation [1-4]. Reptation is characterized by one-dimensional Rouse-like [3-5] curvilinear diffusion in an entanglement tube formed by the topological constraints of surrounding chains. The relevant distance scale for this motion therefore lies between the limits of the interentanglement distance, a, and the polymer rms end-to-end length, $\bar{R}$, and is typically in the range 50 to 5000 Å. Corresponding with these lengths is the time taken to diffuse distance a, the equilibration time, τ_e, and the time taken to diffuse distance $\bar{R}$ in the laboratory frame, the tube disengagement time, τ_d. τ_e and τ_d are typically in the range nanoseconds to seconds.

One means of describing the polymer motion is via the rms laboratory frame displacement of the polymer segments [3],

$$\phi(t) = \langle [\mathbf{R}_n(t) - \mathbf{R}_n(0)]^2 \rangle . \tag{1}$$

The characteristic behavior of $\phi(t)$ over the various time regimes represents a signature for reptative motion, namely [3], (I) free Rouse motion

$$t \lesssim \tau_e,\ \ \phi(t) \lesssim a^2,\ \ \phi(t) \sim t^{1/2}; \tag{2a}$$

(II) Rouse motion constrained to the tube

$$\tau_e \lesssim t \lesssim \tau_R,\ \ a^2 \lesssim \phi(t) \lesssim \bar{R}a,\ \ \phi(t) \sim t^{1/4}; \tag{2b}$$

(III) curvilinear diffusion in the tube

$$\tau_R \lesssim t \lesssim \tau_d,\ \ \bar{R}a \lesssim \phi(t) \lesssim \bar{R}^2,\ \ \phi(t) \sim t^{1/2}; \tag{2c}$$

(IV) long-range center-of-mass motion

$$\tau_d \lesssim t,\ \ \bar{R}^2 \lesssim \phi(t),\ \ \phi(t) \sim t . \tag{2d}$$

τ_R is the Rouse time. Whereas I refers to local, segmental Rouse motion, II and III refer to the motion of the primitive chain. Note that the transition regions from II to III and from III to IV occur at approximately $3\pi^2\tau_R$ and $\pi\tau_d$, respectively. Regime IV corresponds to polymer self-diffusion with coefficient D_s. The tube disengagement time τ_d can be calculated from $\bar{R}$ and D_s via [3]

$$\tau_d = \bar{R}^2/3\pi^2 D_s . \tag{3}$$

Using the tube diameter a, one can calculate Z, the number of steps in the primitive path,

$$Z = \bar{R}^2/a^2 \tag{4a}$$

and hence

$$\tau_R = \tau_d/3Z . \tag{4b}$$

To date most experimental tests of reptation have focused on the molar mass scaling law, $D_s \sim M^{-2}$, which results from Eq. (3). While there is substantial evidence for M^{-2} scaling in polymer melts [6], such scaling has by no means been established in the case of a semidilute solution [4]. Of critical importance to the reptation picture is the existence of sufficient numbers of entanglements to justify a mean-field description. Most studies of self-diffusion in a semidilute solution have employed polymers with molar masses below 1×10^6 daltons for which the tube diameter a is comparable with the polymer dimension $\bar{R}$. Consequently, it is highly doubtful whether the entanglement tube exists for such systems.

Furthermore, the existence of an M^{-2} scaling region is not unique to the reptation model and cannot therefore be regarded as the definitive signature for this motion even when the molar mass is sufficiently high that $Z \gg 1$. A more convincing test is to examine the entire motional regime of the polymer, and especially the internal modes represented by regimes II and III above [7]. To measure $\phi(t)$ requires a technique sensitive to self-motion over the distance regime 50 to 5000 Å and the correspondingly appropriate time scales as defined above. Traditionally, such a measurement would be made via the dynamic self-motion structure factor in a scattering experiment, namely,

$$E(\mathbf{q},t) = N^{-1} \sum \langle \exp\{i2\pi\mathbf{q} \cdot [\mathbf{R}_n(t) - \mathbf{R}_n(0)]\} \rangle . \tag{5}$$

The leading term in the power-series expansion of $E(\mathbf{q},t)$ is $-2\pi^2 q^2 \langle z(t)^2 \rangle$ where $3\langle z(t)^2 \rangle = \phi(t)$ and q is the magnitude of $\mathbf{q}$. Currently the two principal techniques used to measure self-motion are neutron scattering (incoherent fraction) and pulsed gradient spin-echo (PGSE) nuclear magnetic resonance (NMR) [8-10] for which Eq. (5) applies in the narrow gradient pulse approximation [9,10]. Unfortunately neutron scattering is confined to measuring $\phi(t) \lesssim 50$ Å while, until recently, PGSE NMR has been confined to $\phi(t) \gtrsim 1000$ Å. Recent improvements [11,12] to the PGSE-NMR method have reduced this lower limit by an order of magnitude. One such method, the PGSE-MASSEY technique [12], is used to obtain results reported here. The time window available to this method is determined by the available gradient amplitude (here 18 $\mathrm{T\,m^{-1}}$) and by spin relaxation. In the present instance it is limited to 10 ms $\lesssim t \lesssim 1$ s.

Figure 1 shows D_s vs M for polystyrene in carbon tetrachloride (CCl_4) at a concentration of 9% (volume fraction). These measurements and all others reported here were performed at 30° C using a PGSE-NMR system operating at 60-MHz proton NMR frequency. Note that in obtaining the data shown in Fig. 1 we have ensured that the diffusion time is sufficiently long for center-of-mass motion, $\phi(t) \sim t$, by utilizing a stimulated echo sequence where necessary. The data are consistent with the usual $D_s \sim M^{-2}$ prediction but due to the limited region of scaling we do not regard such behavior as convincing.

For the $\phi(t)$ vs t experiments we have chosen a high molar mass subset using M values in excess of 1×10^6 daltons and varied the observation times over the widest possible range. Using literature values of $\bar{R}$ and the D_s data of Fig. 1, Doi-Edwards theory [3] can be used to generate the parameters shown in Table I. Note that in the case of the 9% 15×10^6 daltons polystyrene sample, where $\tau_d \approx 10$ s, the self-diffusion coefficient in region IV cannot be measured directly and we use Fig. 1 to obtain D_s by extrapolation assuming $D_s \sim M^{-2}$. The minimum numbers of entanglements are calculated by assuming $a \lesssim 320$ Å for the 9% solutions, a choice which we shall subsequently justify. Using this upper limit we may calculate the number of primitive path steps Z using Eq. (4). The values of $Z \gtrsim 10$ represent sufficient entanglements for the tube model to apply [13] for these polymer solutions. It should also be noted that three of the calculated tube disengagement times cause $\pi\tau_d$ to lie within the experimental time window of PGSE NMR.

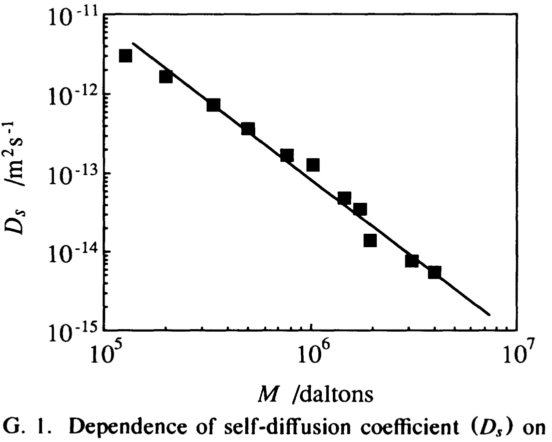

FIG. 1. Dependence of self-diffusion coefficient (D_s) on molar mass (M) for polystyrene in CCl_4 at 9% volume fraction. The straight line corresponds to $D_s \sim M^{-2}$ and has been used to obtain D_s for the 15×10^6 daltons sample by extrapolation.

TABLE I. Parameters relating to polymer systems used in this work calculated using Eqs. (3) and (4). Polystyrenes were obtained from Polymer Laboratories (Shropshire, England) with molar masses (and polydispersity parameters) of 15×10^6 (1.25), 3.04×10^6 (1.04), and 1.75×10^6 (1.06). $\bar{R}$ values were obtained from concentration-dependent radii for polystyrene in CS_2 [14] for which the dilute solution coil expansion factor is approximately 1.7, the same as in CCl_4 [14,15].

M_p	Volume fraction (%)	$\bar{R}$ (Å)	D_s ($\mathrm{m^2s^{-1}}$)	a (Å)	Z	τ_d (s)	τ_R (ms)
15×10^6	9	2900	3.5×10^{-6}[a]	320	82	8.1	33
3.0×10^6	9	1300	7.5×10^{-15}	320	17	0.076	1.5
1.8×10^6	9	990	3.5×10^{-14}	320	10	0.010	0.33
15×10^6	2.2	3100	6.5×10^{-14}	930[b]	11	0.050	1.5
15×10^6	13	2700	1.5×10^{-16}[c]	280	93	16	58

[a]Extrapolated from M^{-2} dependence.
[b]Extrapolated from $c^{-0.75}$ dependence.
[c]Extrapolated from c^{-3} dependence.

Figure 2 shows $\phi(t)$ vs t obtained from the low-q dependence of $E(q,t)$ [i.e., $E(q,t)$, $t \gtrsim 0.5$] for four of the polymer solutions of Table I. While Fig. 2(a) compares the data with scaling lines for $t^{1/4}$, $t^{1/2}$, and t behavior, in Fig. 2(b) the data are compared with the numerical predictions of the Doi-Edwards theory [2,3]. A transition region from $\phi(t) \sim t$ to $\phi(t) \sim t^{1/2}$ is clearly visible for three of the four polymer systems as the observation time is reduced below 1 s. In each case the position of this transition closely agrees with the theoretical reptation prediction. For the 15×10^6 daltons polystyrene at 9% concentration no such transition is apparent, consistent with our calculated value of τ_d. It is important to note that, in the region $t \gtrsim \tau_R$, the theoretical curves of Fig. 2(b) contain no adjustable parameters and use only the empirical D_s and $\bar{R}$ values shown in Table I. The chosen value of a is significant only in the region $t \lesssim \tau_R$.

The transition from $\phi(t) \sim t^{1/2}$ to $\phi(t) \sim t^{1/4}$ would be expected in the vicinity $t \sim 3\pi^2\tau_R$, and at a length scale $\bar{R}a$. Reference to Table I indicates that, given the chosen upper limit values of a, we would expect to just see this transition within the PGSE-NMR time scale only for the 9% solution of 3.0×10^6 daltons polystyrene and the 2.2% solution of 15×10^6 daltons polystyrene in CCl_4. Our data do not clearly indicate such a transition for these polymer systems, suggesting that a is somewhat smaller than the chosen maximum. However, we do see a clear

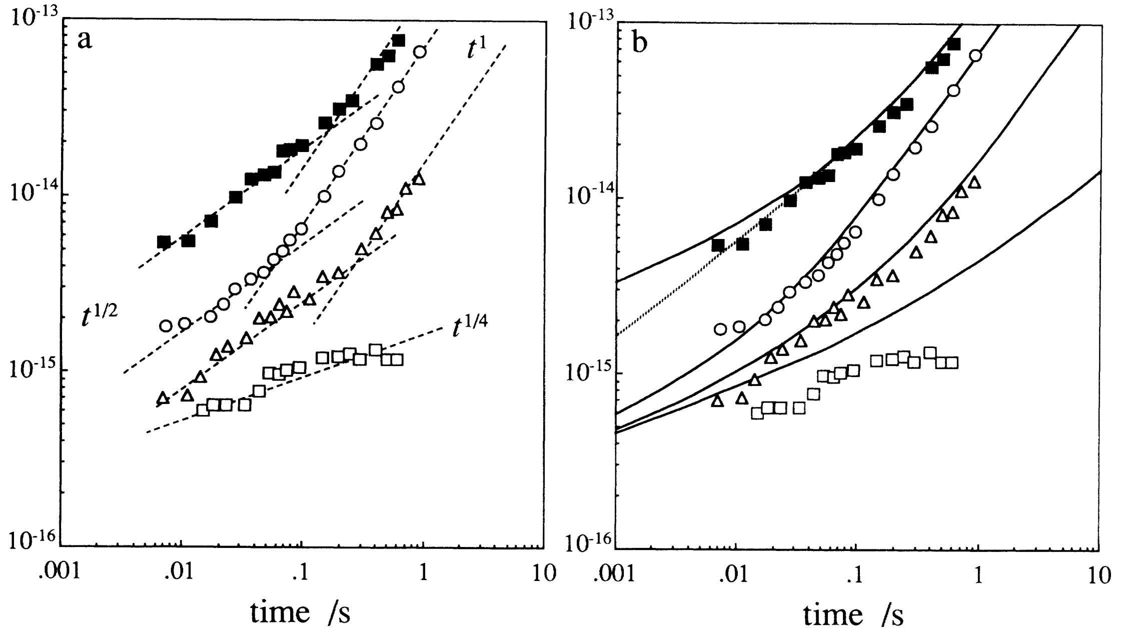

FIG. 2. $\langle z(t)^2 \rangle$ vs t data for polystyrene in CCl_4 (solid squares 2.2% 15×10^6 daltons, open circles 9% 1.8×10^6 daltons, open triangles 9% 3.0×10^6 daltons, open squares 9% 15×10^6 daltons). Note that $\phi(t)=3\langle z(t)^2\rangle$, z being the component of displacement along q. (a) The data are compared with asymptotic lines for $t^{1/4}$, $t^{1/2}$, and t scaling. (b) The solid curves correspond to Doi-Edwards theory for regions II, III, and IV, calculated using the parameters of Table I. For the 2.2% 15×10^6 daltons system the effect of the transition from II to III is shown in the upper solid curve whereas the lower dashed line corresponds to the Doi-Edwards prediction incorporating only regions III and IV.

$t^{1/4}$ region in the case of the 9% solution of 15×10^6 daltons polystyrene, although the absolute values of the mean-square displacements are somewhat below the predictions of Doi-Edwards theory based on the value of D_s extrapolated for this polymer. It should be noted that the theory represents the data well if a value of D_s is chosen which is a factor of 5 lower. This casts some doubt on the use of M^{-2} scaling to obtain D_s by extrapolation.

One other prediction of the Doi-Edwards theory is that the $\phi(t)$ vs t data for a common tube diameter should converge at $\phi(\tau_e)\approx a^2$. For the three sets of data corresponding to different molar masses with a common solution concentration, and hence tube diameter, a high degree of convergence is apparent at short observation times. We note that the convergence value of $\langle z(t)^2\rangle$ is $\lesssim 3\times10^{-16}$ m^2, consistent with the maximum value of a assumed here.

So far we have considered only the motion of the primitive chain measured using the low-q limit of Eq. (5). Superposed on this is the rapid Rouse motion about the primitive chain which occurs at distance scales shorter than a. To examine this "local" motion it is necessary to measure the high-q dependence of $E(\mathbf{q},t)$. The incoherent dynamic structure factor of Eq. (5) represents the Fourier transform of the average propagator [16] of the motion. We shall find it convenient to treat the local motion and the longer-range primitive chain motion as stochastically independent so that the total average propagator is a convolution of local and primitive chain propagators. In consequence the overall dynamic structure factor will be a product of factors for the local and primitive chain motions.

Because the PGSE-NMR observation time greatly exceeds τ_e, the average propagator for this local motion is an autocorrelation function of the polymer segments density distribution, $\rho_l(\mathbf{r})$, in their motion transverse to the tube. This leads to a structure factor $|S_l(\mathbf{q})|^2$, where $S_l(\mathbf{q})$ is the Fourier transform of $\rho_l(\mathbf{r})$ [17]. Consequently,

$$E(\mathbf{q},t)=|S_l(\mathbf{q})|^2 E_{\text{pc}}(\mathbf{q},t)\,, \tag{6}$$

where $E_{\text{pc}}(\mathbf{q},t)$ is the primitive chain dynamic structure factor. A suitable choice for $\rho_l(\mathbf{r})$ is the Gaussian distribution, $(2\pi\sigma)^{-1/2}\exp(-\mathbf{r}^2/2\sigma^2)$ where 2σ may be regarded as the tube diameter. This would lead to $|S_l(\mathbf{q})|^2$ of $\exp(-4\pi^2\mathbf{q}^2\sigma^2)$. $E_{\text{pc}}(\mathbf{q},t)$ is given by the Doi-Edwards theory [2] for regions III and IV but we are unaware of any analytic expression for the region II incoherent structure factor. For the purpose of interpreting $|S_l(\mathbf{q})|^2$ we therefore use the extrapolated region III $E_{\text{pc}}(\mathbf{q},t)$ dynamic structure factor as an approximation.

Figure 3 shows $E(q,t)$ vs q^2, for 15×10^6 polystyrene per CCl_4 solutions at 9% and 13% concentrations, obtained at a fixed measurement time of 48.5 ms. Also shown are the corresponding $E_{\text{pc}}(q,t)$ curves calculated using values of $\overline{R}$ and D_s given in Table I. The concave

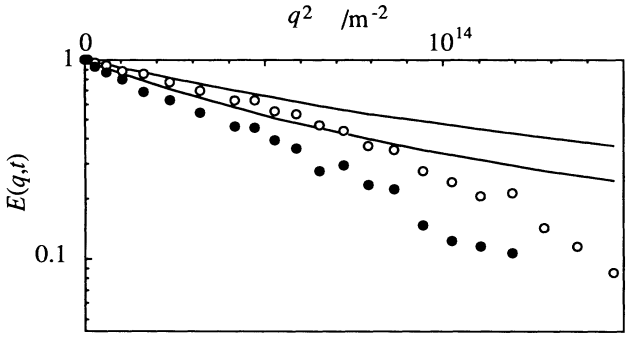

FIG. 3. $E(q,t)$ vs q^2 for 15×10^6 daltons polystyrene at 9% (open circles) and 13% (solid circles) in CCl_4. The observation time t is 48.5 ms, sufficiently long for the PGSE narrow pulse approximation to hold. The theoretical lines correspond to Doi-Edwards incoherent structure factors and the downwards deviation of the data at high q is believed to arise from time-averaged local Rouse motion restricted within the entanglement tube.

nature of $E_{pc}(q,t)$ vs q^2 permits the observation of $|S_1(q)|^2$ attenuation provided $qa\sim1$. From the e^{-1} points of this additional attenuation we estimate tube diameter values of 320 and 280 Å for the 9% and 13% solutions. At best these values are rough estimates. We note that their ratio is not consistent with the static $c^{-0.75}$ dependence, a fact which may reflect hydrodynamic influences [18]. A more detailed analysis would require an accurate description of $E_{pc}(q,t)$ over the entire range of q employed here. However, the present data enable us to set upper limits on a. Both the $E(q,t)$ vs q^2 data and the $\phi(t)$ vs t data are consistent with a tube diameter smaller than 320 Å for the 9% solutions.

It should be emphasized that the q values used here are unusually large for PGSE NMR [$2\pi q\sim(130\ \text{Å})^{-1}$] and that the data reliability depends on the echo-stabilizing effect of the PGSE-MASSEY technique. In the event that the additional attenuation evident at high q contains an instrumental artifact, we may take the values of a determined here as upper limits. While our conclusions regarding magnitude to the tube diameters in semidilute solution are somewhat tentative, the establishment of these maximum values lends credence to the tube depiction for the very high molar mass polymer solutions used in this work.

By contrast we attach a high degree of significance to the $\phi(t)$ vs t observations shown in Fig. 2. While such transitional behavior has been found in computer simulations [19–22], to our knowledge, these data represent the first direct measurement of the motional regimes long considered a signature for reptation.

---

[1] P. G. de Gennes, J. Chem. Phys. **55**, 572 (1971).

[2] M. Doi and S. F. Edwards, J. Chem. Soc. Faraday Trans. II **74**, 1789 (1978).

[3] M. Doi and S. F. Edwards, *The Theory of Polymer Dynamics* (Oxford Univ. Press, Oxford, 1987).

[4] T. P. Lodge, N. A. Rotstein, and S. Prager, Adv. Chem. Phys. **74**, 1 (1990).

[5] P. E. Rouse, J. Chem. Phys. **21**, 1272 (1953).

[6] P. F. Green and E. J. Kramer, Macromolecules **19**, 1108 (1986).

[7] D. Richter, B. Farago, L. J. Fetters, J. S. Huang, B. Ewen, and C. Lartigue, Phys. Rev. Lett. **64**, 1389 (1990).

[8] E. O. Stejskal and J. E. Tanner, J. Chem. Phys. **42**, 288 (1965).

[9] E. O. Stejskal, J. Chem. Phys. **43**, 3597 (1965).

[10] P. T. Callaghan, *Principles of Nuclear Magnetic Resonance Microscopy* (Oxford Univ. Press, Oxford, 1991).

[11] R. Kimmich, W. Unrath, G. Schnur, and E. Rommel, J. Magn. Reson. **91**, 136 (1991).

[12] P. T. Callaghan, J. Magn. Reson. **88**, 493 (1990).

[13] K. Kremer and G. S. Grest, J. Phys. Condens. Matter **2A**, 295 (1990).

[14] J. Des Cloizeaux and G. Jannink, *Polymers in Solution* (Oxford Univ. Press, Oxford, 1990).

[15] P. T. Callaghan and D. N. Pinder, Macromolecules **14**, 1334 (1981).

[16] J. Kärger and W. Heink, J. Magn. Reson. **51**, 1 (1983).

[17] P. T. Callaghan, A. Coy, D. MacGowan, K. J. Packer, and F. O. Zelaya, Nature (London) **351**, 467 (1991).

[18] W. Paul, K. Binder, D. W. Heermann, and K. Kremer, J. Phys. (France) II **1**, 37 (1991).

[19] K. E. Evans and S. F. Edwards, J. Chem. Soc. Faraday Trans. II **77**, 1891 (1981).

[20] J. M. Deutsch, Phys. Rev. Lett. **49**, 926 (1982).

[21] A. Baumgartner, Annu. Rev. Phys. Chem. **35**, 419 (1984).

[22] K. Kremer, G. S. Grest, and I. Carmesin, Phys. Rev. Lett. **61**, 566 (1988).